Unique Cardiac Purkinje Fiber Transient Outward Current β-Subunit Composition:

A Potential Molecular Link to Idiopathic Ventricular Fibrillation

Ling Xiao, **Tamara T. Koopmann**, **Balázs Ördög**, **Pieter G. Postema**, **Arie O. Verkerk**, **Vivek Iyer**, **Kevin J. Sampson**, **Gerard J.J. Boink**, **Maya A. Mamarbachi**, **Andras Varro**, **Luc Jordaens**, **Jan Res**, **Robert S. Kass**, **Arthur A. Wilde**, **C.R. Bezzina**, and **Stanley Nattel**

Department of Medicine, Montreal Heart Institute and Université de Montréal, Montreal, QC, Canada (L.X., B.O., M.A.M., S.N.); Department of Clinical and Experimental Cardiology (T.T.K., P.G.P., G.J..J.B., A.A.W., C.R.B.) and Department of Anatomy, Embryology and Physiology (A.O.V.), Heart Failure Research Center, Academic Medical Center, Amsterdam, the Netherlands; Department of Pharmacology, College of Physicians and Surgeons of Columbia University, New York, NY (V.I., K.J.S., R.S.K.); Department of Pharmacology and Pharmacotherapy, University of Szeged, Szeged, Hungary (A.V.); and Department of Cardiology, Thorax Centre, Erasmus University Rotterdam, Rotterdam, the Netherlands (L.J., J.R.)

Abstract

Rationale—A chromosomal haplotype producing cardiac overexpression of dipeptidyl peptidase-like protein-6 (DPP6) causes familial idiopathic ventricular fibrillation. The molecular basis of transient outward current (I_{to}) in Purkinje fibers (PFs) is poorly understood. We hypothesized that DPP6 contributes to PF I_{to} and that its overexpression might specifically alter PF I_{to} properties and repolarization.

Objective—To assess the potential role of DPP6 in PF I_{to}.

Methods and Results—Clinical data in 5 idiopathic ventricular fibrillation patients suggested arrhythmia origin in the PF-conducting system. PF and ventricular muscle I_{to} had similar density, but PF I_{to} differed from ventricular muscle in having tetraethylammonium sensitivity and slower recovery. DPP6 overexpression significantly increased, whereas DPP6 knockdown reduced, I_{to} density and tetraethylammonium sensitivity in canine PF but not in ventricular muscle cells. The K⁺-channel interacting β-subunit K⁺-channel interacting protein type-2, essential for normal expression of I_{to} in ventricular muscle, was weakly expressed in human PFs, whereas DPP6 and frequenin (neuronal calcium sensor-1) were enriched. Heterologous expression of Kv4.3 in Chinese hamster ovary cells produced small I_{to}; I_{to} amplitude was greatly enhanced by coexpression with K⁺-channel interacting protein type-2 or DPP6. Coexpression of DPP6 with

Correspondence to Stanley Nattel, Université de Montréal, 5000 Belanger St E, Montreal, QC, H1T 1C8, Canada. stanley.nattel@icm-mhi.org.

Author Manuscript

Kv4.3 and K$^+$-channel interacting protein type-2 failed to alter I_{to} compared with Kv4.3/K$^+$-channel interacting protein type-2 alone, but DPP6 expression with Kv4.3 and neuronal calcium sensor-1 (to mimic PF I_{to} composition) greatly enhanced I_{to} compared with Kv4.3/neuronal calcium sensor-1 and recapitulated characteristic PF kinetic/pharmacological properties. A mathematical model of cardiac PF action potentials showed that I_{to} enhancement can greatly accelerate PF repolarization.

Conclusions—These results point to a previously unknown central role of DPP6 in PF I_{to}, with DPP6 gain of function selectively enhancing PF current, and suggest that a DPP6-mediated PF early-repolarization syndrome might be a novel molecular paradigm for some forms of idiopathic ventricular fibrillation.

Keywords

cardiac arrhythmia mechanisms; ECG; genetic arrhythmia syndromes; molecular electrophysiology; potassium channels; sudden death; ventricular tachycardia arrhythmia

Sudden cardiac death accounts for 300 000 deaths annually in North America.[1,2] Almost 10% of patients with sudden cardiac death lack identifiable heart disease, manifesting so-called idiopathic ventricular fibrillation (IVF).[3] The mechanisms underlying most IVF are unknown. Recently, a genome-wide haplotype-sharing analysis of Dutch families with IVF identified a founder haplotype on chromosome 7 (7q36), harboring the proximal and upstream sequences of the *DPP6* gene as the genetic basis.[4] IVF patients with this haplotype had markedly (~20-fold) increased cardiac tissue levels of *DPP6* mRNA.[4]

Dipeptidyl aminopeptidase-like protein-6 (DPP6), a member of the dipeptidyl aminopeptidase family lacking enzymatic activity, is a potential β-subunit for neuronal A-type currents[5,6] and cardiac transient outward potassium current (I_{to})[7] encoded by Kv4.x-subunits. DPP6 modulates trafficking, kinetics, and pharmacology of Kv4.x-encoded channels.[6–8] I_{to} underlies the early-repolarization phase of cardiac action potentials (APs)[9] and shows marked transmural variability.[10] Alterations in myocardial I_{to} expression play important roles in cardiac arrhythmias[11] and have been implicated in Brugada syndrome, although precise mechanisms remain controversial.[12]

Cardiac Purkinje fibers (PFs) form a specialized conducting system, with unique properties and important roles in cardiac physiology and arrhythmia generation.[13] There are major differences in I_{to} between ventricular muscle (VM) and PFs in many species, including humans.[13,14] PF I_{to} typically shows slower inactivation and much greater tetraethylammonium (TEA) sensitivity than VM.[13,14] The molecular mechanisms underlying these differences are unclear. The β-subunit K$^+$-channel interacting protein type-2 (KChIP2), which plays a crucial role in VM I_{to}, is weakly expressed in PF.[15] In addition to KChIP2 and DPP6, other potential Kv4.2/4.3-interacting subunits include neuronal calcium sensor-1 (NCS-1) and KCNE1–5,[16–19] many of which are expressed in the heart.[20] DPP6 is known to confer TEA sensitivity on Kv4.x-subunit– based channels on heterologous expression.[8] We hypothesized that DPP6 may contribute to PF I_{to} and that its overexpression might alter PF I_{to} properties in a way that contributes to IVF occurrence. The present study was designed (1) to assess the expression of various β-subunits in human VM

and PF tissue, (2) to evaluate the result of DPP6 overexpression and knockdown by adenoviral gene transfer on VM and PF I_{to}, and (3) to study the properties of I_{to} resulting from heterologous coexpression of different combinations of putative β-subunits relevant to composition in human VM and PF. Our results point to an important contribution of DPP6 to PF I_{to} and implicate enhanced PF I_{to} as a novel candidate mechanism for IVF.

Methods

For further details, see the online Data Supplement.

Clinical Assessment of IVF Patients

Five IVF patients with confirmed 7q36 DPP6–associated haplotype were studied. Baseline clinical data were obtained for all. One patient underwent invasive electrophysiological study and long-term follow-up.

Human Cardiac Tissue Samples

Hearts from 15 nondiseased donors (8 for mRNA and 7 for protein extraction) were stored in cardioplegic solution at 4°C. PF false tendons, left ventricular (LV) epicardium, midmyocardium, and endocardium were dissected and snap-frozen in liquid N_2.

mRNA Quantifcation

RNA was extracted with TRIzol, chlorofiorm extraction, and isopropanol precipitation. Genomic DNA was eliminated with DNase I, followed by phenol-chlorofiorm acid. First-strand cDNA was synthesized by reverse transcription with 1 μg RNA, random primers, and moloney murine leukemia virus reverse transcriptase. Real-time polymerase chain reaction was conducted (primers are given in Online Table I) with SYBR green. 18S rRNA was the internal standard. mRNA was quantified with comparative threshold cycle quantification (Ct).

Immunoblotting

Membrane protein fractions were run on 10% SDS-PAGE gels and transferred to polyvinylidene fluoride membranes. Blots were probed with primary antibodies against Kv4.3, KChIP2, NCS-1, DPP6, and GAPDH. Results were analyzed with Quantity-One, and data were normalized to GAPDH.

Native-Cell Isolation and Culture

Experiments were performed with canine cardiac tissues, which have relative VM and PF cell (PC) I_{to} properties similar to those of humans.[13,14] Adult male mongrel dogs (19–30 kg, n=33) were anesthetized with pentobarbital (30 mg/kg IV). After excision of PF false tendons, the anterior LV (or in selected experiments, right ventricular [RV] free wall) was arterially perfused with Tyrode solution containing collagenase (120 U/mL, Worthington, type II). VM cardiomyocytes were isolated as previously described.[21] PCs were obtained by digestion with elastase and collagenase (for details, see Online Methods). Isolated cells were either put in storage solution for study on the same day or placed in cell culture on laminin-coated glass coverslips. In some cases, attached PCs and VMs were subjected to adenovirus

infection for 2 to 4 hours and incubated for 48 hours. After culture, PCs and VMs were washed and stored at 4°C for electrophysiological study.

Adenovirus Constructs

A bicistronic construct encoding triple FLAG-tagged DPP6 and green fluorescent protein (GFP) under control of the cytomegalovirus promoter was generated by inserting the cDNA into pShuttle-IRES-hrGFP-1 vector. The adenoviral vector containing DPP6 cDNA is designated Adv-GFP-DPP6, and the control vector containing only GFP is designated Adv-GFP-control.

DPP6 knockdown was obtained with a microRNA-embedded short-hairpin RNA (shRNA-mir[57]) sequence, targeted to the canine DPP6 mRNA (GeneBank identification, XM_532774). The shRNA-mir sequence was delivered into the cultured cells by a human adenovirus-based vector (Adv-GFP-DPP6-knockdown). A scrambled shRNA-mir carrying adenovirus was used as a negative control (Adv-GFP-Scr). KChIP2 knockdown virus and a scrambled control construct were prepared similarly. Adenovirus vector construction followed previous studies.[22,23] For details, see online Data Supplement Methods. GFP expression was used to select cells with effective gene transfer.

Chinese Hamster Ovary Cell Culture and Transfection

Chinese hamster ovary (CHO) cells were cultured in F12-medium supplemented with bovine serum and penicillin/streptomycin. Transfection was performed with Lipofectamine 2000 and plasmid DNA encoding Kv4.3 or combinations of Kv4.3 with KChIP2b, DPP6, or NCS-1. Bicistronic vectors carrying DsRed, cyan fluorescence protein, and GFP were used to monitor gene transfer. Fluorescent cells were used for patch-clamp experiments within 1 to 2 days of transfection.

Immunoprecipitation Studies

Total proteins from CHO cells after 2-day transfections extracted with lysis buffer were fast-frozen and stored at −80°C. Immunoprecipitation was performed with a monoclonal anti-Kv4.3 antibody. Dynabeads M-280/sheep antimouse IgG were washed with PBS and preincubated with 1% BSA for 1 hour at room temperature to minimize nonspecific binding. Anti-Kv4.3 antibodies were incubated overnight at 4°C with 100 μL Dynabeads per sample. The anti-mouse IgG-coated beads were then washed 5 times with PBS and incubated overnight with 100 μg protein extracts from CHO cells, and supernatants were collected. The bead–antibody target protein complexes were washed and subjected to magnetic precipitation/resuspension. Bound Kv4.3 protein complexes were eluted and denatured.

Eluted proteins and supernatants were separated on 10% SDS-PAGE gel and transferred to polyvinylidene fluoride membranes. Blots were incubated overnight at 4°C with primary antibodies against Kv4.3, KChIP2, NCS-1, or DPP6. Protein bands were detected by chemiluminescence, and results were analyzed with Quantity-one software.

Confocal Microscopy

Two days after transfection, CHO cells were washed with PBS, then fixed with 2% paraformaldehyde, and washed 3 times with PBS. After blocking and permeabilization, cells were incubated overnight at 4°C with primary antibody against Kv4.3 in PBS containing 1% normal donkey serum and 0.05% Triton, followed by 3 washes and incubation with secondary antibody and wheatgerm agglutinin. Confocal microscopy was performed with a Zeiss LSM-710 system. Images were deconvolved using measured point-spread functions. Kv4.3 fluorescence densities were determined as the sum of the pixels within each region normalized to region area. Measurements were repeated in 5 Z stacks for each cell.

Electrophysiology

Whole-cell patch-clamp technique was applied for I_{to} recording at 36±0.5°C (native cells) or 22±0.5°C (CHO cells). I_{to} was always defined as the difference between peak and end-pulse current. Cell capacitances were not significantly different among groups (Online Table II). Recording solutions were as previously described[14–16] (see online Data Supplement).

Data Analysis

Clampfit 9.0 (Axon) and GraphPad Prism 5.0 were used for basic data analysis. Real-time polymerase chain reaction results were analyzed with MXPro software. Statistical comparisons were performed with paired or unpaired Student *t* tests for 2-group-only analysis and by ANOVA followed by Bonferroni-corrected *t* tests for multiple-group comparisons. A 2-tailed value of $P<0.05$ indicated statistical significance; group data are mean±SEM.

PF AP Model

A previously described model of the electrophysiology of the PF cell was used,[24] modified to reproduce behavior of canine cell recordings at physiological temperature. Current density was set to reproduce a peak current of 10 pA/pF at 30 mV.[25]

Results

IVF Patients

Baseline ECGs were normal in *DPP6* risk-haplotype carriers (Online Table III). Ventricular arrhythmia manifested as short coupled ventricular extrasystoles (VESs) that sometimes initiated rapid polymorphic ventricular tachyarrhythmias (Online Figure I). VESs consistently displayed left bundle-branch block morphology and superior/leftward ECG axis, suggesting a lower RV origin. The short VES coupling intervals despite normal QTc, along with the relatively narrow QRS complexes, suggest an origin in the conduction system, as observed by Haïssaguerre et al[26] in 25% of their IVF patients. In 1 patient undergoing ablation for repeated arrhythmia storm after implantation of a cardioverter-defibrillator (Figure 1), RV pace mapping produced a morphology similar to that of VESs (Figure 1A and 1B). Radiofrequency ablation was applied at a site with early diastolic PF potentials (Figure 1C) in the anterior lower RV (Figure 1D). During the 43-month follow-up, neither ventricular fibrillation nor typicalmorphology VESs occurred.

Differences Between PC and VM I_{to}

Figure 2A and 2B shows examples of I_{to} in freshly isolated canine PCs and VMs. The currents have similar overall morphologies, with PCs showing somewhat slower inactivation and larger end-pulse sustained currents compared with VM. Both PC I_{to} and VM I_{to} are completely blocked by 10 mmol/L 4-aminopyridine (Online Figure II). Overall current densities are of the same order for PCs and VMs (Figure 2C and 2D). Both PF I_{to} and VM I_{to} show biexponential inactivation (Figure 2E); however, the slow-phase inactivation time constants were slower for PF (Figure 2F and 2G). For example, the time constants at 30 mV averaged 8.3±1.0 milliseconds (fast phase) for PF versus 4.6±0.4 milliseconds for VM (P=0.005), and the slow-phase time constants averaged 66.5±15.4 milliseconds for PF versus 13.5±2.0 milliseconds for VM (P=0.044). The relative proportion of inactivation attributable to fast-phase inactivation was smaller in PF (57±6%) compared with VM (72±2%; P<0.05).

Figure 3 shows inactivation voltage dependence and recovery kinetics for PCs versus VM. Inactivation voltage dependence (Figure 3A and 3B) tended to be less negative in PCs: 50% inactivation voltages were −28.5±0.6 mV (PF) versus −34.0±2.8 mV (VM; P=0.184). Fast-phase recovery time constants were similar: 30±5 milliseconds for PF versus 21±4 milliseconds for VM (P=NS), but slow-phase recovery time constants were much slower for PF (691±139 milliseconds) compared with VM (166±48 milliseconds; P=0.04). The slow phase also comprised a larger portion of total inactivation in PF, 61±6%, compared with VM (39±7%; P=0.04). I_{to} properties were stable over 2 days in culture (Figures 2 and 3).

A signature property of PC I_{to} is TEA sensitivity.[13,14] PC and VM responses to TEA (10 mmol/L) are illustrated in Figure 4A and 4B. TEA 10 mmol/L reduced PC I_{to} by ≈50% at 50 mV (Figure 4C). The dose-response relation for TEA inhibition of fresh PC I_{to} (Online Figure IIIA) showed a 50% inhibitory concentration (IC_{50}) of 2.0±1.6 mmol/L. Neither inactivation time constants (Online Figure IIIB) nor the percentage of fast-versus slow-phase inactivation was changed by 100 mmol/L TEA. Recovery was accelerated by 10 mmol/L TEA (Online Figure IIIC) because of a decrease in the slow-phase proportion from 77±4% to 41±3% (P<0.01) without any change in the time constants per se. In contrast, VM I_{to} was unaffected by 10 mmol/L TEA (Figure 4D) and non-significantly decreased with 100 mmol/L TEA (Online Figure IIID). The relative responses of PCs versus VMs were unchanged after a 2-day culture (Figure 4E and 4F).

All VM studies described above were performed in LV cells. We also compared PC I_{to} properties with those of RV cardiomyocytes. RV I_{to} was insensitive to 10 mmol/L TEA (Online Figure IVA), quite different from PCs (Online Figure IVB). Similar to LV VM, RV I_{to} inactived faster than PC (Online Figure VA and VB). The voltage dependence of I_{to} inactivation was less negative for PC I_{to} compared with RV (Online Figure VC). Recovery kinetics were also faster in RV cardiomyocytes compared with PCs (Online Figure VD). Overall, differences between PCs and RV cardiomyocytes paralleled those for LV cardiomyocytes.

Effects of DPP6 Expression Changes on PC and VM I_{to}

To assess the effect of DPP6 overexpression, as occurs in 7q36-IVF, on PC and VM I_{to}, we used adenovirus-based DPP6 gene transfer (Figure 5A and 5B). DPP6 overexpression significantly increased both I_{to} density (by ≈52%; Figure 5C) and TEA sensitivity (Figure 5D) in PCs but did not alter current density (Figure 5E) or TEA sensitivity (Figure 5F) in VMs. DPP6 overexpression did not alter I_{to} inactivation kinetics or voltage dependence (Online Figure VI). The time course of recovery from inactivation was similarly unaffected by DPP6 overexpression (Online Figure VII). Effective overexpression was confirmed at the mRNA level (Online Figure VIIIA).

To further assess the potential role of DPP6 in PC and VM I_{to}, we studied the effects of DPP6 knockdown on native I_{to}. Effective DPP6 knockdown was confirmed by measuring DPP6 mRNA (online Figure VIIIB). Examples of I_{to} in PCs and VMs infected with the scrambled control and DPP6-knockdown virus are shown in Figure 6A and 6B. DPP6 knockdown significantly decreased PC I_{to} density (Figure 6C) and TEA sensitivity (Figure 6D) but did not affect VM I_{to} (Figure 6E and 6F). Inactivation kinetics and voltage dependence, recovery kinetics, and relative amplitudes were not affected by DPP6 knockdown for both PC and VM I_{to} (Online Figure IX).

Purkinje Fiber Versus Myocardial Expression of I_{to}-Related Subunits

The studies shown in Figures 5 and 6 support the contention that DPP6 is an important contributor to PC (but not VM) I_{to}. To evaluate potential underlying mechanisms, we first assessed the differential expression of potential I_{to} subunits in PFs and VMs. Normal human hearts presented marked DPP6 mRNA expression gradients between PF and LV (Figure 7A). DPP6 mRNA expression was 29±10-, 23±7-, and 15±5-fold higher in PF compared wtih LV epicardium, midmyocardium, and endocardium, respectively (Figure 7A, inset). Kv4.3, Kv3.4, and Kv1.4 were similarly expressed in PF and LV, with Kv4.3 expression being by far the strongest. KChIP2b expression in LV epicardium was ≈5-fold greater than in PF, whereas NCS-1 was more strongly expressed (≈4-fold) in PF. KCNE1, KCNE2, and KCNE3 mRNA levels were not differential. We also measured the expression of Kv4.3, KChIP2, NCS-1, and DPP6 proteins in PF and VM membrane preparations from normal human hearts (Figure 7B and 7D) and from canine hearts (Figure 7C and 7E). The protein expression differences for Kv4.3, KChIP2, NCS-1, and DPP6 in PF and VM qualitatively paralleled relative transcript expression (Figure 7A), with KChIP2 more strongly expressed in VM and NCS-1 and DPP6 more strongly expressed in PF. Kv4.3 protein levels were not significantly different between PF and VM. Membrane extracts from CHO cells overexpressing the various subunits studied were probed with the antibodies used, showing good selectivity (Online Figure X).

Effects of β-Subunit Background on Heterologously Expressed Kv4.3

To relate the different properties of VM compared with PF I_{to} to the various subunits they express, we studied the effects of DPP6 on Kv4.3+KChIP2 (mimicking VM I_{to} subunit makeup) or Kv4.3+NCS-1 (mimicking PC I_{to} subunit makeup) in CHO cells. Figure 8A through 8F shows representative I_{to} recordings from CHO cells transfected with Kv4.3 alone, Kv4.3+KChIP2, Kv4.3+KChIP2+DPP6, Kv4.3+NCS-1, Kv4.3+NCS-1+DPP6, or

Kv4.3+DPP6. Corresponding mean current density data are shown in Figure 8G. KChIP2 enhanced I_{to} current density (Figure 8B versus 8A), but the addition of DPP6 produced no further change (Figure 8C and 8G). NCS-1 cotransfection with Kv4.3 increased I_{to} slightly compared with Kv4.3 alone (Figure 8D), and the addition of DPP6 substantially enhanced I_{to} (Figure 8E). DPP6 alone enhanced I_{to} to about the same extent as DPP6 in the presence of NCS-1 (Figure 8F and 8G). Changes in mean inactivation time constants are shown in Figure 8H, with illustrative fits in Figure 8I. Currents encoded by Kv4.3+KChIP2 or Kv4.3+NCS-1 inactivated more slowly than Kv4.3-only current. Coexpression of DPP6 with Kv4.3+KChIP2 or with Kv4.3 alone did not significantly alter the rate of inactivation. However, τ_{inact} for currents encoded by Kv4.3+NCS-1+DPP6 was similar to τ_{inact} of Kv4.3+NCS-1 currents and slower than for Kv4.3+KChIP2 ($P<0.05$) or Kv4.3 alone. The voltage dependence of Kv4.3 inactivation was left-shifted by coexpression with DPP6 only but was not significantly altered by cotransfection with the other subunit combinations studied (Online Figure XIA and Online Table IV).

Changes in subunit composition significantly affected I_{to} recovery (Figure 8J and Online Figure XIB). Cells transfected with Kv4.3 alone had slower recovery time constants than cells cotransfected with Kv4.3+KChIP2. Adding DPP6 to Kv4.3+KChIP2 did not significantly alter recovery kinetics compared with Kv4.3+KChIP2. Cotransfection of Kv4.3 with NCS-1, with or without DPP6, slowed recovery $\approx$3-fold relative to K4.3+KChIP2. Cotransfection of Kv4.3 with DPP6 alone accelerated Kv4.3 recovery to an extent similar to that of KChIP2.

Subunit composition significantly affected TEA sensitivity. Currents recorded before and after 5 mmol/L TEA in cells transfected with Kv4.3 alone and Kv4.3+DPP6 are shown in Online Figure XIIA and XIIB, respectively. Online Figure XIIC shows mean percentage inhibition by 5 mmol/L TEA of cells transfected with Kv4.3 and various combinations of β-subunits. Cells transfected with Kv4.3 alone, Kv4.3+KChIP2, and Kv4.3+KChIP2+DPP6 showed no significant effect of TEA. NCS-1 conferred slight TEA sensitivity. Cotransfection of DPP6 with Kv4.3 alone or with Kv4.3+NCS-1 significantly enhanced TEA sensitivity relative to Kv4.3+NCS-1. TEA sensitivity of cells cotransfected with Kv4.3+NCS-1+DPP6 was not significantly different from Kv4.3+DPP6. Thus, DPP6 enhances Kv4.3 currents and TEA sensitivity only in the absence of KChIP2.

Although the expression data do indicate stronger DPP6 expression in PF compared with VM, the protein data indicate relatively small quantitative rather than the qualitative differences seen with mRNA. We therefore considered the possibility that the prominent role of DPP6 in PF might be the result of interference with DPP6-Kv4.3 interaction by KChIP2, the predominant I_{to} β-subunit in VM that is weakly expressed in PCs, based on the lack of change in current density when DPP6 is added to Kv4.3+KChIP2 (Figure 8G) and the inability of DPP6 to induce TEA sensitivity when cotransfected with Kv4.3+KChIP2 (Online Figure XIIC). To study the physical interaction of various combinations of β-subunits with Kv4.3, we immunoprecipitated proteins from CHO cells expressing Kv4.3, Kv4.3+KChIP2, Kv4.3+KChIP2+DPP6, Kv4.3+DPP6, Kv4.3+NCS-1, or Kv4.3+NCS-1+DPP6 with a monoclonal anti-Kv4.3 antibody (Online Figure XIIIA). Kv4.3 was effectively and completely precipitated from each group because the 75-kDa Kv4.3

band was not observed in the supernatants. The 115-kDa DPP6 band was detected in the immunoprecipitates obtained from Kv4.3+KChIP2+DPP6, Kv4.3+DPP6, and Kv4.3+NCS-1+DPP6. Not all expressed DPP6 protein was bound to Kv4.3 because it was also detected in the supernatant. KChIP2 and NCS-1 similarly coimmunoprecipitated with Kv4.3, with significant amounts remaining in the supernatant. The amount of DPP6 that coimmunoprecipitated with Kv4.3 was significantly less when KChIP2 was expressed together with Kv4.3 and DPP6 compared with Kv4.3+DPP6 without KChIP2 (Online Figure XIIIB).

Potential Basis for Kv4.3 Current Enhancement by KChIP2 and DPP6

Either KChIP2 or DPP6 substantially enhances K4.3 current. To gain insights into possible mechanisms, we assessed CHO cell Kv4.3 expression in plasma membranes by immunohistochemistry (Online Figure XIV) and in crude membrane preparations with Western blot (Online Figure XV). Both approaches suggest that KChIP2 or DPP6 increases Kv4.3 membrane expression.

Effects of KChIP2 Knockdown on VM I_{to}

If KChIP2 prevents Kv4.3-DPP6 interaction and VM has significant DPP6 expression, DPP6 might be able to maintain Kv4.3 function when KChIP2 levels are decreased. To test this possibility, we knocked KChIP2 down with adenoviral gene transfer in VMs. Examples of I_{to} from VMs infected with scrambled control and KChIP2-knockdown viruses are shown in Online Figure XVIA. Effective KChIP2 knockdown was confirmed by an ≈50% decrease in KChIP2 Western blot signal (Online Figure XVIB). KChIP2 knockdown did not significantly affect I_{to} density (Online Figure XVIC).

Effects of Increased I_{to} on PC APs in a Mathematical Model

Our studies of the properties of PFs versus VM, of the effect of DPP6 overexpression and knockdown on native PCs and VMs, of putative I_{to} subunit composition, and of the results of cotransfection of Kv4.3 with different subunit combinations in CHO cells all point to an important role of DPP6 in PF I_{to} composition and suggest that increased DPP6 expression enhances PF I_{to}. We then sought to understand the potential functional consequences of DPP6 overexpression. We were unable to record physiological APs from cultured PCs. We therefore turned to a previously described computational model of the PC AP.[24] Online Figure XVIIA shows the baseline model-derived I_{to}. The effects of I_{to} overexpression on PF repolarization are shown in Online Figure XVIIB. Increasing degrees of upregulation cause progressive deepening of the phase 1 notch and shortening of AP duration, leading to loss of the AP plateau and early repolarization directly from phase 1.

Discussion

The recent discovery of a founder risk haplotype on chromosome 7q36, which includes the proximal and upstream regions of the *DPP6* gene, in Dutch familial IVF subjects brought the potential for new insights into our understanding of the mechanisms underlying IVF.[4] In risk-haplotype carriers, IVF is highly linked to cardiac overexpression of the *DPP6* gene,[4] pointing to increased DPP6 expression as a potential molecular basis. However, the link

between *DPP6* upregulation and arrhythmogenesis has been unclear. In the present study, we examined clinical data from 5 *DPP6* risk-haplotype carriers who had suffered IVF and found that *DPP6*-related IVF arrhythmias likely originated from the PF system. In nondiseased human hearts, we observed that DPP6 is more richly expressed in PFs compared with its expression in VMs. Besides DPP6, we found PF-VM differences in the expression of KChIP2 and NCS-1, with KChIP2 being more abundant in VMs and sparse in PFs, whereas NCS-1 is more strongly expressed in PFs than VMs. The biophysical and pharmacological properties of PF I_{to} are known to differ from those of VM I_{to},[13,14] but the underlying molecular mechanism has been unknown. In addition, the basis for substantial PF I_{to} density has been mysterious, in light of weak PF expression of KChIP2,[15] known to be essential for VM I_{to} expression.[27] The data presented here suggest that DPP6 performs a function in PFs comparable to that of KChIP2 in VMs, permitting normal current expression of I_{to}. In addition, NCS-1 and DPP6 recapitulated the specific functional PF I_{to} phenotype when coexpressed with the α-subunit Kv4.3, and DPP6 knockdown suppressed native PC I_{to}. Overexpression of DPP6 to mimic the particular cardiac gene expression phenotype observed in IVF patients enhances PF (but not VM) I_{to}; in vivo, this would translate into accelerated PF repolarization, which might cause a form of PF early-repolarization syndrome.

Possible Role in Arrhythmogenesis

Cardiac PFs participate in the initiation and maintenance of ventricular arrhythmias in the presence of pathology like congestive heart failure or myocardial infarction or in inheritable arrhythmic syndromes like the long-QT syndrome.[28–31] They have also been implicated in catecholaminergic polymorphic ventricular tachycardia.[32] PFs are particularly susceptible to early afterdepolarizations or delayed afterdepolarizations.[33,34] Ion channel remodeling in PFs contributes to arrhythmogenic electrophysiological abnormalities in diseased hearts.[14,24,35–37] Our discovery that upregulation of *DPP6* expression specifically enhances I_{to} in cardiac PF but not VM is the first mechanistic clue to the pathogenesis of *DPP6*-related IVF. The absence of alterations in ventricular I_{to} with DPP6 overexpression potentially explains the normal ECG in risk-haplotype carriers because the Purkinje system is a small fraction of the myocardial mass.

Imbalances between I_{to} and inward currents have been suggested to underlie the development of ventricular arrhythmias. *KCND3* (encoding Kv4.3) or *KCNE3* gain-of-function mutations seen in Brugada syndrome patients enhance ventricular I_{to} and are presumed to cause steep transmural repolarization gradients that induce spontaneous generation of ectopic beats.[38,39] In the risk haplotype for IVF, increased Purkinje I_{to} expression with *DPP6* enhancement might similarly deepen phase 1 and appreciably accelerate repolarization (Online Figure XVII). Accelerated PF repolarization could cause strong local repolarization gradients with adjacent ventricular muscle (unaffected by DPP6 overexpression), thereby generating local ectopic activity that produces early coupled VESs without other evidence of electrocardiographic early-repolarization syndromes. This interesting possibility remains to be tested directly.

I_{to} Subunit Composition and Properties

The TEA sensitivity of PF I_{to} was a classic observation that contributed to the recognition that I_{to} is carried predominantly by K^+.[40] In contrast, VM I_{to} is TEA insensitive.[13,14] Similarly, I_{to} recovery is markedly slower in PFs compared with VM,[13,14] contributing to well-established differences in AP rate responsiveness.[41] Nevertheless, the molecular basis for Purkinje I_{to} has not been established despite studies of PF I_{to}-related subunit composition.[15,20,42,43] In addition to permitting normal I_{to} densities in the virtual absence of KChIP2, the sub-unit profiles we noted here may account for the unique TEA sensitivity and kinetic properties of PF I_{to}: DPP6 bequeathing TEA sensitivity and NCS-1 slow recovery. In previous studies, we found higher levels of Kv3.4 in PFs than in VM (findings we could not confirm here), identifying Kv3.4 as a potential contributor to Purkinje I_{to}.[15] However, the TEA sensitivity of Kv3 channels is an order of magnitude greater than that of Purkinje I_{to}, and high concentrations of blood-depressing substance, a potent and specific Kv3.4 channel blocker, fail to inhibit Purkinje I_{to}.[13] The results here present for the first time a plausible basis for the previously enigmatic molecular composition of Purkinje I_{to}.

KChIP2 and NCS-1 are members of the recoverin/NCS subfamily of calcium-binding proteins.[44,45] Both proteins can interact with Kv4 channels and are recognized as regulatory subunits for Kv4 subunit channels in neuron and myocardium.[5,10,16,17,44,45] The specific role of NCS-1 in the heart has not been determined. Nakamura et al[16] initially suggested that NCS-1 regulates K4 currents. Guo et al[17] showed that NCS-1 is expressed in mammalian myocardium, slows Kv4 current inactivation, and enhances current density. In mouse, NCS-1 is developmentally regulated and more abundant in immature hearts.[45] Relatively little is known about the regional distribution of NCS-1 expression. Greener et al[42] found greater frequenin (NCS-1) mRNA levels in the bundle of His (composed of PCs) than in VM. Extremely low-level KChIP2 expression in PFs is a consistent finding.[15,20,42,43,46] Our finding of greater PF DPP6 abundance compared with VM is consistent with other recent observations.[42,43] The interaction of DPP6 with Kv4.x subunits is also known to facilitate subunit trafficking and to alter current kinetics.[5,6,8,47] The effect of DPP6 on Kv4 subunit channel TEA sensitivity is related to modified TEA binding to the external side of the pore.[8,48] Our coexpression studies suggest that both NCS-1 and DPP6 contribute to the properties of PF I_{to}, with DPP6 required to enhance Kv4.3 current density and TEA sensitivity and NCS-1 necessary for the typical kinetic properties (slower inactivation and recovery). These observations provide new insights into the functional importance of differential PF-VM I_{to} subunit expression profiles.

Potential Limitations

In this study, we developed a novel in vitro system of cultured PCs and applied it to study the consequences of DPP6 overexpression, as seen in IVF, for PF I_{to}. We were unable to record physiologically relevant APs from cultured PCs, which prevented us from directly assessing the impact of DPP6 overexpression on PC APs. Instead, we used a mathematical PC-AP model to analyze the effect of PF I_{to} gain of function. Further work is needed to explore the electrophysiological phenotype associated with DPP6 overexpression. Because of the brief murine AP, studies in transgenic models more closely related to humans such as

the rabbit[49] may be needed. Interspecies differences in I_{to} also exist between the human and canine heart[50] and need to be considered in the assessment of the application of our findings.

We compared I_{to} kinetics in native PCs and VMs with identical 100-millisecond depolarizing pulse protocols (Figure 3). Although these studies allowed us to demonstrate slower I_{to} inactivation in PCs compared with VM, because of the slow nature of PC I_{to} recovery, the slow-phase time constants could not be accurately quantified with such short pulses. We subsequently used a 1-second depolarizing pulse protocol and obtained results suggesting that the slow-phase time constant is at least on the order of 400 milliseconds (Online Figure XVIII).

Our DPP6 overexpression and knockdown data indicate that DPP6 plays a significant role in PF but not in VM I_{to}, but our studies do not establish a clear molecular basis for this highly PF-selective contribution. DPP6 and NCS-1 are more strongly expressed in human PF than VM at both the protein and mRNA levels (Figure 2); however, the PF-VM discrepancy is much greater in mRNA than protein expression. The mRNA data are more strictly quantitative than the protein data but are further removed from the functional molecule. The protein data are based on membrane preparations that include a variety of cell membranes and not solely the sarcolemma; in addition, the protein data do not reflect compartmentalization in potentially critical macromolecular complexes. Western blot analyses are limited by imperfect specificity and the detection of multiple molecular weight bands, particularly for polyclonal antibodies. KChIP2 seems to prevent Kv4.3 interaction with DPP6, as reflected by the lack of Kv4.3 current increase with DPP6 in the presence of KChIP2 compared with KChIP2-Kv4.3 alone (Figure 8G), the inability of DPP6 to confer TEA sensitivity in the presence of KChIP2 (Online Figure XIIC), and the reduction in DPP6 physical interaction with Kv4.3 in the presence of KChIP2 (Online Figure XIII). Thus, the low-level expression of KChIP2 in PF may contribute at least as much to the manifest role of DPP6 as the PF-VM differences in DPP6 expression per se. In contrast, coexpression with NCS-1 does not interfere with any DPP6 effects and is required to reproduce slow PC recovery kinetics. It must be noted that although our study clarifies the basis of unusual PF I_{to} properties by suggesting that the characteristic slowly recovering and TEA-sensitive components are likely caused by the involvement of NCS-1 and DPP6, by indicating that PF I_{to} current amplitude is maintained by DPP6 in the relative absence of KChIP2, and by pointing to PF early repo-larization as a mediator of arrhythmogenic consequences of DPP6-overexpressing arrhythmia syndromes, many questions about the molecular composition of PF I_{to} remain unanswered and need to be addressed in future work. It is likely that PF I_{to} consists of >1 channel type because TEA blocked a maximum of ≈75% of the current and selectively suppressed the slowly recovering kinetic component.

Studies in native cells are essential to assess the composition of native channels but are limited by the variability introduced by varying cell quality and ionic current densities. For this reason, we were as careful as possible to study all groups and interventions within each series of experiments in contemporaneous experiments and whenever possible within each set of cells. We studied native-cell properties at a physiological temperature (36°C) to work under as physiological conditions as possible. However, currents in heterologously expressing cells were too large at 36°C to be effectively voltage clamped. Therefore,

heterologous cell work was done at room temperature, greatly slowing current kinetics. Comparisons with native-cell data are therefore based on qualitative findings rather than quantitative comparisons between corresponding kinetic components.

Translational Relevance

Our study is the first to address the pathophysiological mechanism of DPP6-related IVF. Familial IVF linked to the chromosome-7 locus including DPP6 presents as a malignant inheritable arrhythmia syndrome.[4,51] The genetic findings enable risk stratifcation,[4,51] and elucidation of the underlying electrophysiological mechanism is important to develop improved treatment. For example, our results provide a potential rationale for the efficacy of quinidine, an I_{to} blocker, in IVF patients, as reported previously.[52] The concepts we elucidated may also aid in understanding potential mechanisms of IVF and in facilitating exploration of mechanisms associated with other novel genes[53] and sudden arrhythmic death paradigms.

Supplementary Material

Refer to Web version on PubMed Central for supplementary material.

Acknowledgments

Nonstandard Abbreviations and Acronyms

AP	action potential
CHO	Chinese hamster ovary
DPP6	dipeptidyl aminopeptidase-like protein-6
GFP	green fluorescent protein
IVF	idiopathic ventricular fibrillation
KChIP2	K^+-channel interacting protein type-2
LV	left ventricle
NCS-1	neuronal calcium sensor-1
PC	Purkinje fiber cell
PF	Purkinje fiber
RV	right ventricle

TEA	tetraethylammonium
VES	ventricular extrasystole
VM	ventricular muscle

References

1. Fishman GI, Chugh SS, Dimarco JP, et al. Sudden cardiac death prediction and prevention: report from a National Heart, Lung, and Blood Institute and Heart Rhythm Society Workshop. Circulation. 2010; 122:2335–2348. [PubMed: 21147730]

2. Zipes DP, Wellens HJ. Sudden cardiac death. Circulation. 1998; 98:2334–2351. [PubMed: 9826323]

3. Survivors of out-of-hospital cardiac arrest with apparently normal heart: need for definition and standardized clinical evaluation: Consensus Statement of the Joint Committees of the Unexplained Cardiac Arrest Registry of Europe and of the Idiopathic Ventricular Fibrillation Registry in the United States. Circulation. 1996; 95:265–272.

4. Alders M, Koopmann TT, Christiaans I, Postema PG, Beekman L, Tanck MW, Zeppenfeld K, Loh P, Koch KT, Demolombe S, Mannens MM, Bezzina CR, Wilde AA. Haplotype-sharing analysis implicates chromosome 7q36 harboring DPP6 in familial idiopathic ventricular fibrillation. Am J Hum Genet. 2009; 84:468–476. [PubMed: 19285295]

5. Maffie J, Rudy B. Weighing the evidence for a ternary protein complex mediating A-type K+ currents in neurons. J Physiol. 2008; 586:5609–5623. [PubMed: 18845608]

6. Nadal MS, Ozaita A, Amarillo Y, Vega-Saenz de Miera E, Ma Y, Mo W, Goldberg EM, Misumi Y, Ikehara Y, Neubert TA, Rudy B. The CD26-related dipeptidyl aminopeptidase-like protein DPPX is a critical component of neuronal A-type K+ channels. Neuron. 2003; 37:449–461. [PubMed: 12575952]

7. Radicke S, Cotella D, Graf EM, Ravens U, Wettwer E. Expression and function of dipeptidyl-aminopeptidase-like protein 6 as a putative beta-subunit of human cardiac transient outward current encoded by Kv4.3. J Physiol. 2005; 565:751–756. [PubMed: 15890703]

8. Colinas O, Pérez-Carretero FD, López-López JR, Pérez-García MT. A role for DPPX modulating external TEA sensitivity of Kv4 channels. J Gen Physiol. 2008; 131:455–471. [PubMed: 18411327]

9. Antzelevitch C. Molecular basis for the transmural distribution of the transient outward current. J Physiol. 2001; 533:1. [PubMed: 11351005]

10. Niwa N, Nerbonne JM. Molecular determinants of cardiac transient outward potassium current (I(to)) expression and regulation. J Mol Cell Cardiol. 2010; 48:12–25. [PubMed: 19619557]

11. Nattel S, Maguy A, Le Bouter S, Yeh YH. Arrhythmogenic ion-channel remodeling in the heart: heart failure, myocardial infarction, and atrial fibrillation. Physiol Rev. 2007; 87:425–456. [PubMed 17429037]

12. Antzelevitch C, Nof E. Brugada syndrome: recent advances and controversies. Curr Cardiol Rep. 2008; 10:376–383. [PubMed: 18715534]

13. Han W, Wang Z, Nattel S. A comparison of transient outward currents in canine cardiac Purkinje cells and ventricular myocytes. Am J Physiol Heart Circ Physiol. 2000; 279:H466–H474. [PubMed: 10924043]

14. Han W, Zhang L, Schram G, Nattel S. Properties of potassium currents in Purkinje cells of failing human hearts. Am J Physiol Heart Circ Physiol. 2002; 283:H2495–H2503. [PubMed: 12388306]

15. Han W, Bao W, Wang Z, Nattel S. Comparison of ion-channel subunit expression in canine cardiac Purkinje fibers and ventricular muscle. Circ Res. 2002; 91:790–797. [PubMed: 12411393]

16. Nakamura TY, Pountney DJ, Ozaita A, Nandi S, Ueda S, Rudy B, Coetzee WA. A role for frequenin, a Ca2+-binding protein, as a regulator of Kv4 K+-currents. Proc Natl Acad Sci U S A. 2001; 98:12808–12813. [PubMed: 11606724]

17. Guo W, Malin SA, Johns DC, Jeromin A, Nerbonne JM. Modulation of Kv4-encoded K(+) currents in the mammalian myocardium by neuronal calcium sensor-1. J Biol Chem. 2002; 277:26436–26443. [PubMed: 11994284]

18. Radicke S, Cotella D, Graf EM, Banse U, Jost N, Varró A, Tseng GN, Ravens U, Wettwer E. Functional modulation of the transient outward current Ito by KCNE beta-subunits and regional distribution in human non-failing and failing hearts. Cardiovasc Res. 2006; 71:695–703. [PubMed: 16876774]

19. Pourrier M, Schram G, Nattel S. Properties, expression and potential roles of cardiac K+ channel accessory subunits: MinK, MiRPs, KChIP, and KChAP. J Membr Biol. 2003; 194:141–152. [PubMed: 14502427]

20. Gaborit N, Le Bouter S, Szuts V, Varro A, Escande D, Nattel S, Demolombe S. Regional and tissue specific transcript signatures of ion channel genes in the non-diseased human heart. J Physiol. 2007; 582:675–693. [PubMed: 17478540]

21. Xiao L, Zhang L, Han W, Wang Z, Nattel S. Sex-based transmural differences in cardiac repolarization and ionic-current properties in canine left ventricles. Am J Physiol Heart Circ Physiol. 2006; 291:H570–H580. [PubMed: 16501015]

22. Paddison PJ, Cleary M, Silva JM, Chang K, Sheth N, Sachidanandam R, Hannon GJ. Cloning of short hairpin RNAs for gene knockdown in mammalian cells. Nat Methods. 2004; 1:163–167. [PubMed: 16144086]

23. Luo J, Deng ZL, Luo X, Tang N, Song WX, Chen J, Sharff KA, Luu HH, Haydon RC, Kinzler KW, Vogelstein B, He TC. A protocol for rapid generation of recombinant adenoviruses using the AdEasy system. Nat Protoc. 2007; 2:1236–1247. [PubMed: 17546019]

24. Sampson KJ, Iyer V, Marks AR, Kass RS. A computational model of Purkinje fibre single cell electrophysiology: implications for the long QT syndrome. J Physiol. 2010; 588:2643–2655. [PubMed: 20498233]

25. Jeck C, Pinto J, Boyden P. Transient outward currents in subendocardial Purkinje myocytes surviving in the infarcted heart. Circulation. 1995; 92:465–473. [PubMed: 7634462]

26. Haïssaguerre M, Shoda M, Jaïs P, et al. Mapping and ablation of idiopathic ventricular fibrillation. Circulation. 2002; 106:962–967. [PubMed: 12186801]

27. Rosati B, Pan Z, Lypen S, Wang HS, Cohen I, Dixon JE, McKinnon D. Regulation of KChIP2 potassium channel beta subunit gene expression underlies the gradient of transient outward current in canine and human ventricle. J Physiol. 2001; 533:119–125. [PubMed: 11351020]

28. Bode K, Hindricks G, Piorkowski C, Sommer P, Janousek J, Dagres N, Arya A. Ablation of polymorphic ventricular tachycardias in patients with structural heart disease. Pacing Clin Electrophysiol. 2008; 31:1585–1591. [PubMed: 19067811]

29. Bogun F, Good E, Reich S, Elmouchi D, Igic P, Tschopp D, Dey S, Wimmer A, Jongnarangsin K, Oral H, Chugh A, Pelosi F, Morady F. Role of Purkinje fibers in post-infarction ventricular tachycardia. J Am Coll Cardiol. 2006; 48:2500–2507. [PubMed: 17174189]

30. Chiang CE, Roden DM. The long QT syndromes: genetic basis and clinical implications. J Am Coll Cardiol. 2000; 36:1–12. [PubMed: 10898405]

31. Ben Caref E, Boutjdir M, Himel HD, El-Sherif N. Role of subendocardial Purkinje network in triggering torsade de pointes arrhythmia in experimental long QT syndrome. Europace. 2008; 10:1218–1223. [PubMed: 18757866]

32. Kang G, Giovannone SF, Liu N, Liu FY, Zhang J, Priori SG, Fishman GI. Purkinje cells from RyR2 mutant mice are highly arrhythmogenic but responsive to targeted therapy. Circ Res. 2010; 107:512–519. [PubMed: 20595652]

33. Nattel S, Quantz MA. Pharmacological response of quinidine induced early afterdepolarisations in canine cardiac Purkinje fibres: insights into underlying ionic mechanisms. Cardiovasc Res. 1988; 22:808–817. [PubMed: 3256422]

34. Maruyama M, Joung B, Tang L, Shinohara T, On YK, Han S, Choi EK, Kim DH, Shen MJ, Weiss JN, Lin SF, Chen PS. Diastolic intracellular calcium-membrane voltage coupling gain and postshock arrhythmias: role of purkinje fibers and triggered activity. Circ Res. 2010; 106:399–408. [PubMed: 19926871]

35. Corrias A, Giles W, Rodriguez B. Ionic mechanisms of electrophysiological properties and repolarization abnormalities in rabbit Purkinje fibers. Am J Physiol Heart Circ Physiol. 2011; 300:H1806–H1813. [PubMed: 21335469]

36. Han W, Chartier D, Li D, Nattel S. Ionic remodeling of cardiac Purkinje cells by congestive heart failure. Circulation. 2001; 104:2095–2100. [PubMed: 11673352]

37. Maguy A, Le Bouter S, Comtois P, Chartier D, Villeneuve L, Wakili R, Nishida K, Nattel S. Ion channel subunit expression changes in cardiac Purkinje fibers: a potential role in conduction abnormalities associated with congestive heart failure. Circ Res. 2009; 104:1113–1122. [PubMed: 19359601]

38. Delpón E, Cordeiro JM, Núñez L, Thomsen PE, Guerchicoff A, Pollevick GD, Wu Y, Kanters JK, Larsen CT, Hofman-Bang J, Burashnikov E, Christiansen M, Antzelevitch C. Functional effects of KCNE3 mutation and its role in the development of Brugada syndrome. Circ Arrhythm Electrophysiol. 2008; 1:209–218. [PubMed: 19122847]

39. Giudicessi JR, Ye D, Tester DJ, Crotti L, Mugione A, Nesterenko VV, Albertson RM, Antzelevitch C, Schwartz PJ, Ackerman MJ. Transient outward current (I(to)) gain-of-function mutations in the KCND3-encoded Kv4.3 potassium channel and Brugada syndrome. Heart Rhythm. 2011; 8:1024–1032. [PubMed: 21349352]

40. Kenyon JL, Gibbons WR. Influence of chloride, potassium, and tetra-ethylammonium on the early outward current of sheep cardiac Purkinje fibers. J Gen Physiol. 1979; 73:117–138. [PubMed: 438768]

41. Miller JP, Wallace AG, Feezor MD. A quantitative comparison of the relation between the shape of the action potential and the pattern of stimulation in canine ventricular muscle and Purkinje fibers. J Mol Cell Cardiol. 1971; 2:3–19. [PubMed: 4106601]

42. Greener ID, Monfredi O, Inada S, Chandler NJ, Tellez JO, Atkinson A, Taube MA, Billeter R, Anderson RH, Efimov IR, Molenaar P, Sigg DC, Sharma V, Boyett MR, Dobrzynski H. Molecular architecture of the human specialised atrioventricular conduction axis. J Mol Cell Cardiol. 2011; 50:642–651. [PubMed: 21256850]

43. Atkinson A, Inada S, Li J, Tellez JO, Yanni J, Sleiman R, Allah EA, Anderson RH, Zhang H, Boyett MR, Dobrzynski H. Anatomical and molecular mapping of the left and right ventricular His-Purkinje conduction networks. J Mol Cell Cardiol. 2011; 51:689–701. [PubMed: 21741388]

44. An WF, Bowlby MR, Betty M, Cao J, Ling HP, Mendoza G, Hinson JW, Mattsson KI, Strassle BW, Trimmer JS, Rhodes KJ. Modulation of A-type potassium channels by a family of calcium sensors. Nature. 2000; 403:553–556. [PubMed: 10676964]

45. Nakamura TY, Sturm E, Pountney DJ, Orenzoff B, Artman M, Coetzee WA. Developmental expression of NCS-1 (frequenin), a regulator of Kv4 K+ channels, in mouse heart. Pediatr Res. 2003; 53:554–557. [PubMed: 12612193]

46. Nattel S, Frelin Y, Gaborit N, Louault C, Demolombe S. Ion-channel mRNA-expression profiling: insights into cardiac remodeling and arrhythmic substrates. J Mol Cell Cardiol. 2010; 48:96–105. [PubMed: 19631654]

47. Radicke S, Cotella D, Sblattero D, Ravens U, Santoro C, Wettwer E. The transmembrane beta-subunits KCNE1, KCNE2, and DPP6 modify pharmacological effects of the antiarrhythmic agent tedisamil on the transient outward current Ito. Naunyn Schmiedebergs Arch Pharmacol. 2009; 379:617–626. [PubMed: 19153714]

48. Wada K, Yokotani N, Hunter C, Doi K, Wenthold RJ, Shimasaki S. Differential expression of two distinct forms of mRNA encoding members of a dipeptidyl aminopeptidase family. Proc Natl Acad Sci U S A. 1992; 89:197–201. [PubMed: 1729689]

49. Brunner M, Peng X, Liu GX, et al. Mechanisms of cardiac arrhythmias and sudden death in transgenic rabbits with long QT syndrome. J Clin Invest. 2008; 118:2246–2259. [PubMed: 18464931]

50. Akar FG, Wu RC, Deschenes I, Armoundas AA, Piacentino V3rd, Houser SR, Tomaselli GF. Phenotypic differences in transient outward K+ current of human and canine ventricular myocytes: insights into molecular composition of ventricular Ito. Am J Physiol Heart Circ Physiol. 2004; 286:H602–H609. [PubMed: 14527940]

51. Postema PG, Christiaans I, Hofman N, Alders M, Koopmann TT, Bezzina CR, Loh P, Zeppenfeld K, Volders PG, Wilde AA. Founder mutations in the Netherlands: familial idiopathic ventricular fibrillation and DPP6. Neth Heart J. 2011; 19:290–296. [PubMed: 21512816]

52. Belhassen B, Viskin S, Fish R, Glick A, Setbon I, Eldar M. Effects of electrophysiologic-guided therapy with Class IA antiarrhythmic drugs on the long-term outcome of patients with idiopathic ventricular fibrillation with or without the Brugada syndrome. J Cardiovasc Electrophysiol. 1999; 10:1301–1312. [PubMed: 10515552]

53. Ohno S, Zankov DP, Ding WG, Itoh H, Makiyama T, Doi T, Shizuta S, Hattori T, Miyamoto A, Naiki N, Hancox JC, Matsuura H, Horie M. KCNE5 (KCNE1L) variants are novel modulators of Brugada syndrome and idiopathic ventricular fibrillation. Circ Arrhythm Electrophysiol. 2011; 4:352–361. [PubMed: 21493962]

Novelty and Significance

What Is Known?

- The specialized ventricular conducting system consists of cardiac Purkinje fiber (PF) cells , which have an unusual form of transient outward K^+ current (I_{to} with particularly slow recovery kinetics.

- In cardiac cells, excessively rapid or excessively slow repolarization can lead to ventricular tachyarrhythmias, potentially lethal cardiac rhythm disturbances.

- A familial idiopathic ventricular fibrillation sudden cardiac death (SCD) syndrome has as its basis a variant gene haplotype that leads to cardiac overexpression of dipeptidyl peptidase-like protein-6 (DPP6), which can act as a subunit component of I_{to}

What New Information Does This Article Contribute?

- SCD patients with the DPP6-overexpressing genotype have ventricular tachyarrhythmias arising in the specialized PF-conducting system.

- DPP6 plays an important role in constituting PF I_{to}, explaining many of its unusual properties and differences from I_{to} elsewhere in the heart.

- DPP6 overexpression enhances PF I_{to}, which can accelerate PF repolarization, and this could explain the clinical idiopathic ventricular fibrillation/SCD syndrome origin in the PF system and the lack of abnormalities in other cardiac regions

PF I_{to} has a number of unusual properties like slow recovery kinetics and high tetraethylammonium sensitivity that suggest a potentially molecular basis distinct from atrial or ventricular muscle. This study assessed the role of DPP6 in PF I_{to} on the basis of evidence that patients with a genetic form of SCD show cardiac DPP6 overexpression, as well as arrhythmias that originate in the PF system. We show that DPP6 is preferentially enriched in PFs and that its overexpression and knockdown enhance and suppress, respectively, I_{to} in PF but not ventricular myocytes. In addition, DPP6 coexpression with the predominant I_{to} pore-forming subunit Kv4.3 alters I_{to} pharmacology, reproducing tetraethylammonium sensitivity. Furthermore, the accessory β-subunit K^+-channel interacting protein type-2, essential for robust I_{to} formation by Kv4.3 subunits in the ventricule, is weakly expressed in PFs, where DPP6 plays a corresponding role in localizing functional Kv4.3 channels to the membrane. A mathematical PF model shows that DPP6 overex-pression–induced I_{to} enhancement can accelerate PF repolarization, potentially leading to ventricular arrhythmogenesis. Our study elucidates the previously cryptic basis for PF I_{to} and introduces a potential new paradigm for idiopathic ventricular fibrillation/SCD. These new insights have the potential to lead to improved understanding and treatment of life-threatening arrhythmias in humans.
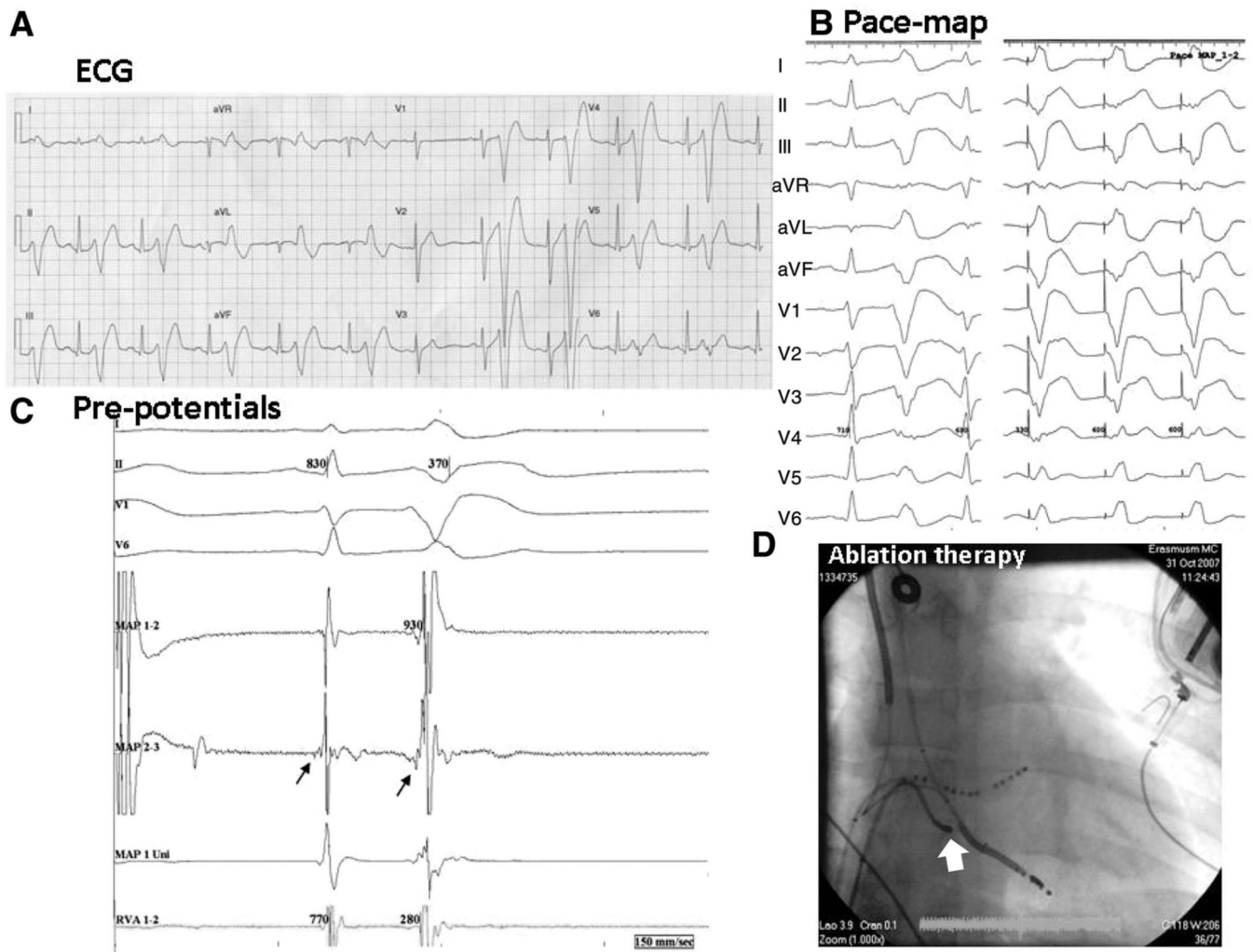
Figure 1. Radiofrequency ablation of idiopathic ventricular fibrillation in a *DPP6* risk-haplotype carrier (patient E)

A, Early coupled ventricular extrasystoles (VESs) with a typical morphology in bigeminal pattern. **B, left**, Spontaneous VES; **right**, the pace map in the right ventricular (RV) apex. **C**, At the ablation site on the mapping ablation catheter, proximal recording (map 2–3) shows an early signal preceding the sinus beat, suggesting a Purkinje potential, which becomes clearer at the onset of a VES. **D**, Catheter position (**arrow**) at a successful ablation site (anteroposterior view). LV indicates left ventricle; and VF, ventricular fibrillation.
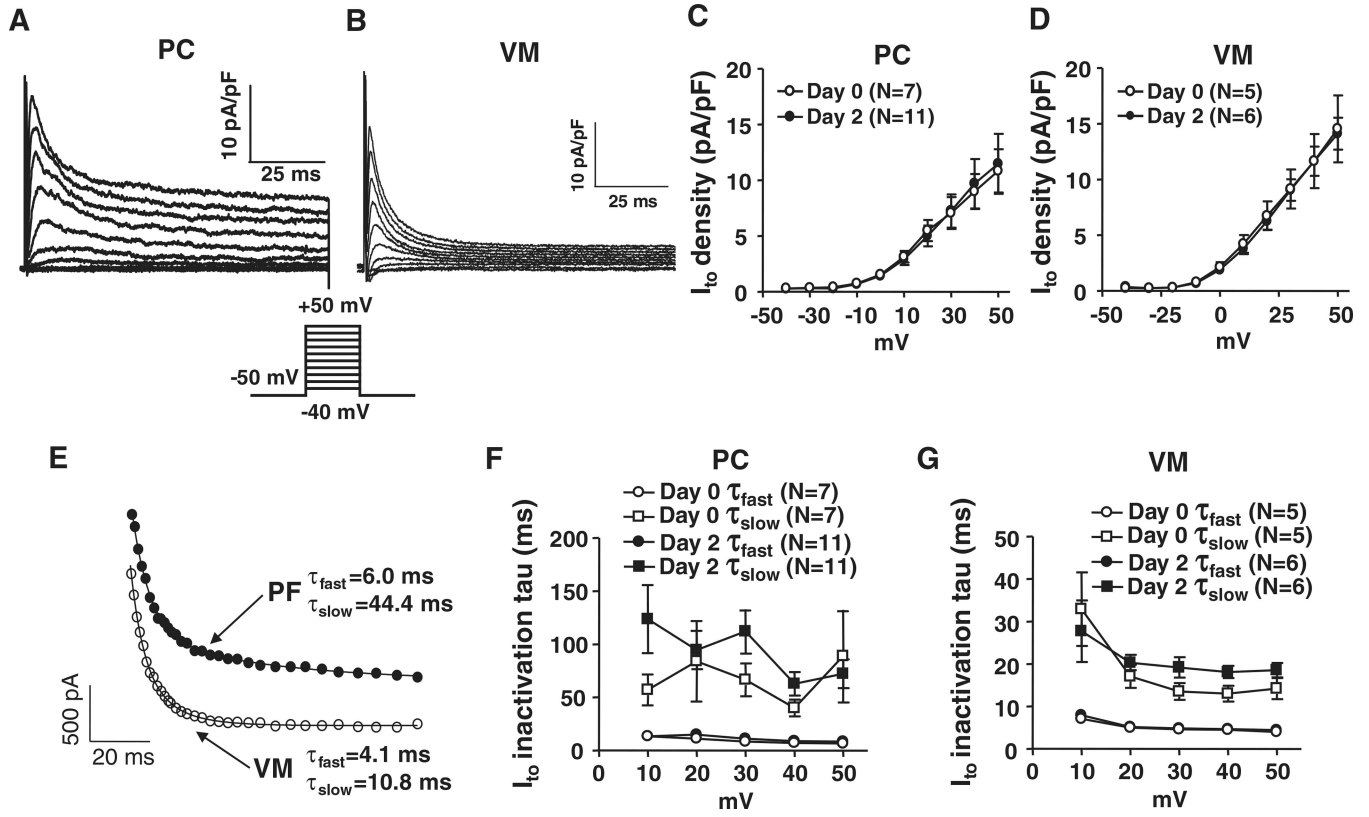
Figure 2. Comparison of I_{to} between Purkinje fiber cells (PCs) and ventricular muscles (VMs)
Representative recordings of I_{to} obtained with 100-millisecond depolarizations from a holding potential of −50 mV at 0.1 Hz in freshly isolated PCs (**A**) or VMs (**B**). **C** and **D**, Mean±SEM I_{to} density-voltage relations at day 0 (freshly isolated) and day 2 culture for PCs and VMs. **E**, Representative best-fit biexponentials to data from a PC and a VM during 100-millisecond depolarizations to 30 mV. **F** and **G**, Mean±SEM I_{to} inactivation time constants.
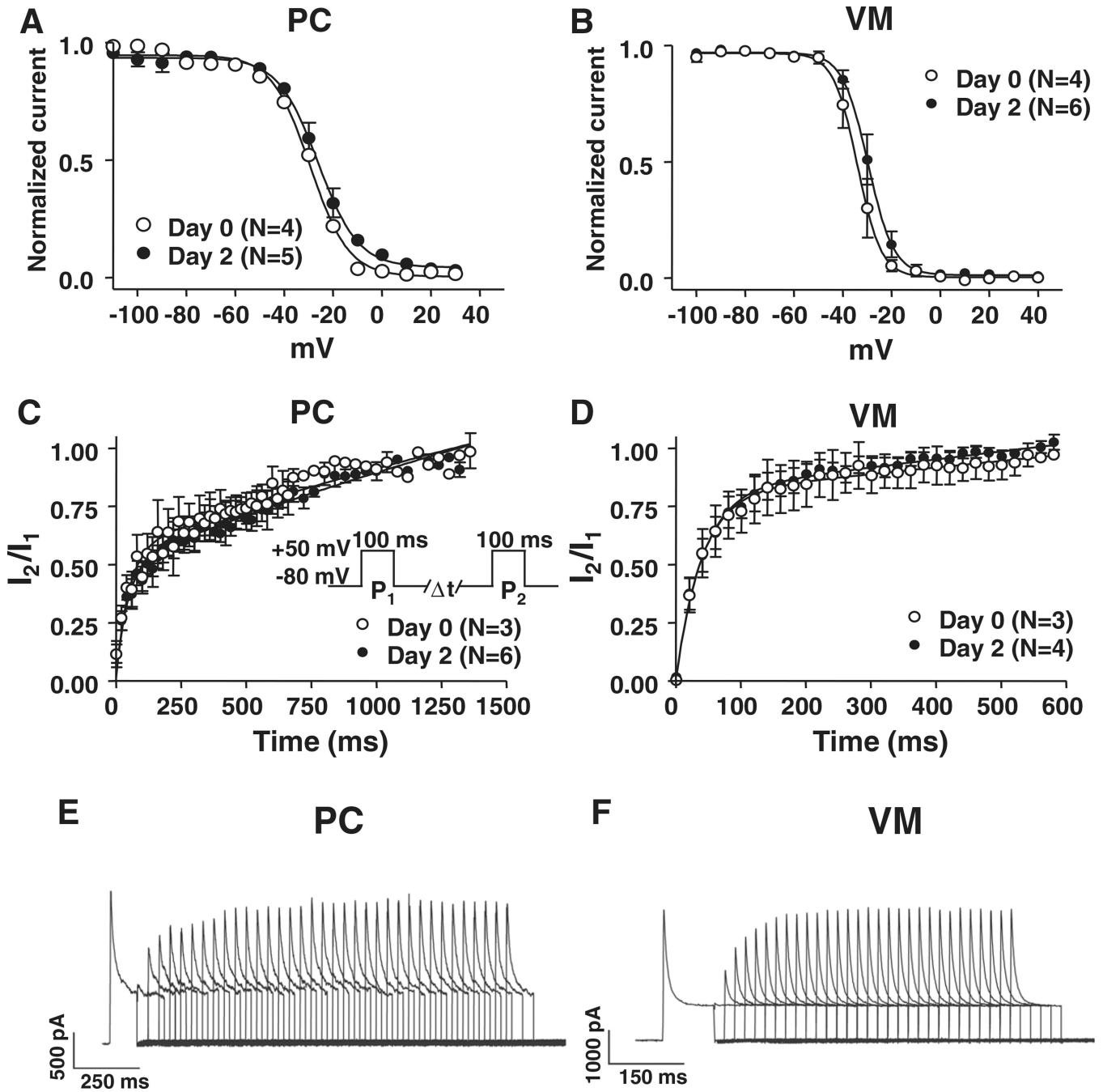
Figure 3. Inactivation voltage dependence and recovery kinetics of Purkinje fiber cell (PC) versus ventricular myocyte (VM) I_to

Mean±SEM voltage dependence of PC (A) and VM (B) Ito inactivation voltage dependence obtained with a 200-millisecond test pulse to 50 mV preceded by 1-second conditioning pulses between −100 and 40 mV. Holding potential is −80 mV. Curves are best-ft Boltzmann relations. **C** and **D**, Time-dependent PC and VM I_{to} recovery from inactivation. Values are mean±SEM I_2/I_1 as a function of P_1–P_2 interval, obtained with the protocol shown in (**C**) at 0.1 Hz. Best-fit biexponential functions are shown. **E** and **F**, Representative

recordings of I_{to} recovery from inactivation in PC and VM. Please note the different time scales.
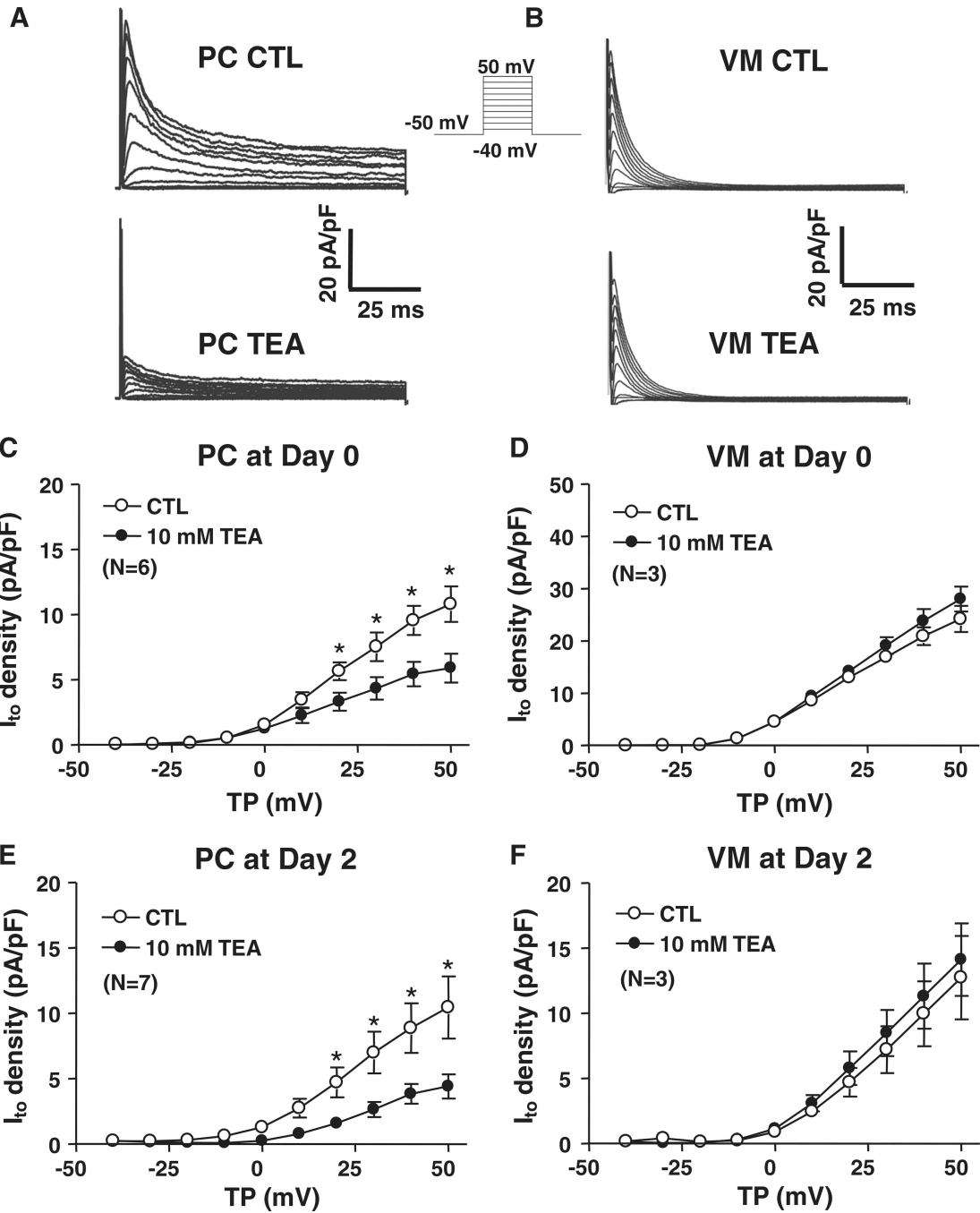
Figure 4. Effects of tetraethylammonium (TEA) on Purkinje fiber cell (PC) and ventricular myocyte (VM) I_{to}

Representative recordings of Ito before (CTL, top) and after (bottom) 10-mmol/L tetraethylammonium (TEA) perfusion in freshly isolated PCs **A**, or VMs **B**. Currents were obtained with 100-millisecond depolarizations from a holding potential of −50 mV at 0.1 Hz. Mean±SEM I_{to} density-voltage relations before and after 10-mmol/L TEA at day 0 (**C** and **D**) and day 2 (**E** and **F**) from PCs (**left**) and VMs (**right**). *$P<0.05$, CTL vs 10 mmol/L TEA. CTL indicates control; TP, test potential.
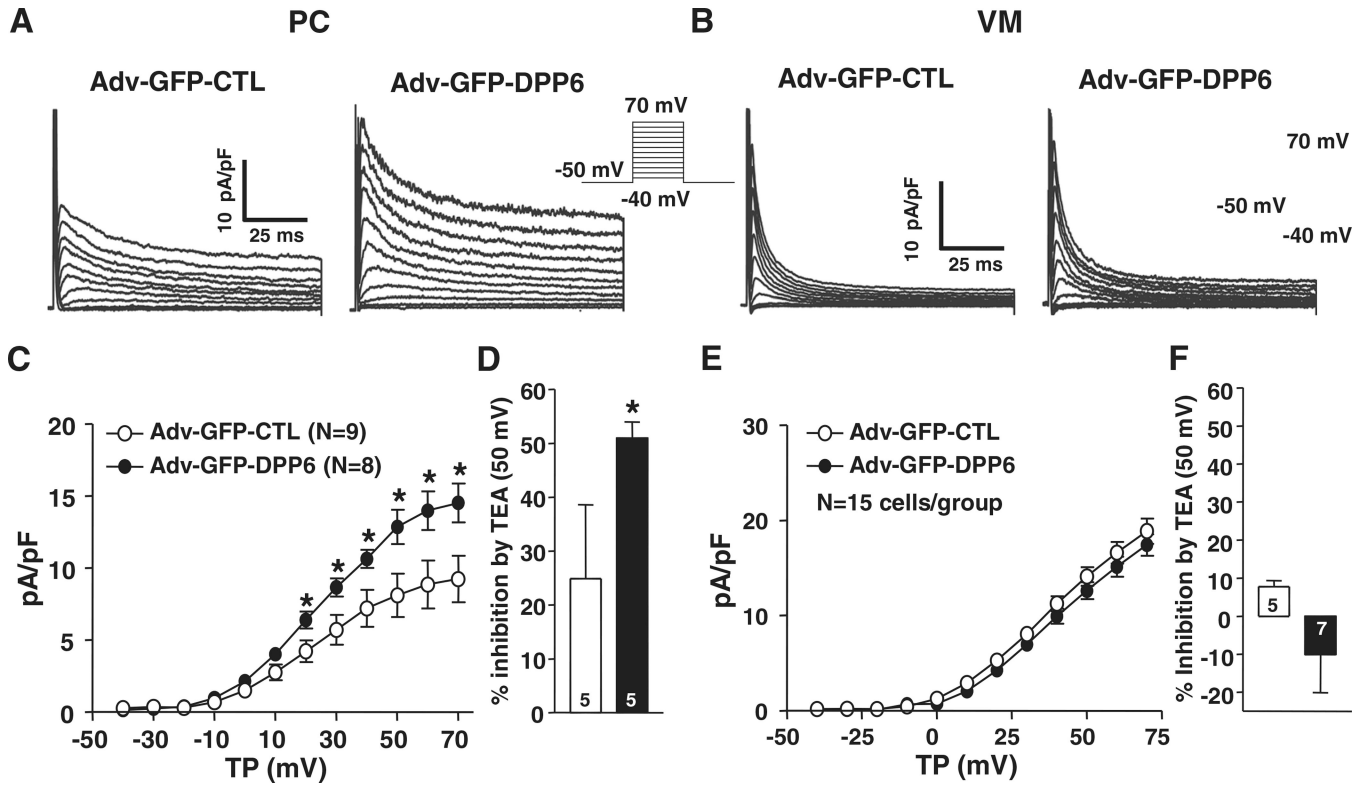
Figure 5. Effects of dipeptidyl peptidase-like protein-6 (DPP6) overexpression on Purkinje fiber cells (PC) and ventricular muscle (VM) I_{to}

A and **B**, I_{to} recordings obtained with 100-millisecond depolarizations from −50 mV at 0.1 Hz in VMs and PCs infected with Adv-GFP-CTL (CTL) or Adv-GFP-DPP6 (DPP6). **C** and **E**, Mean±SEM I_{to} density-voltage relations in CTL or DPP6 from VMs (**C**) and PCs (**E**). **D** and **F**, Percentage inhibition by 10 mmol/L tetraethylammonium (TEA) of VM (**D**) or PC (**F**) I_{to} at 50 mV. *$P<0.05$, CTL vs DPP6. GFP indicates green fluorescent protein; and T P, test potential.
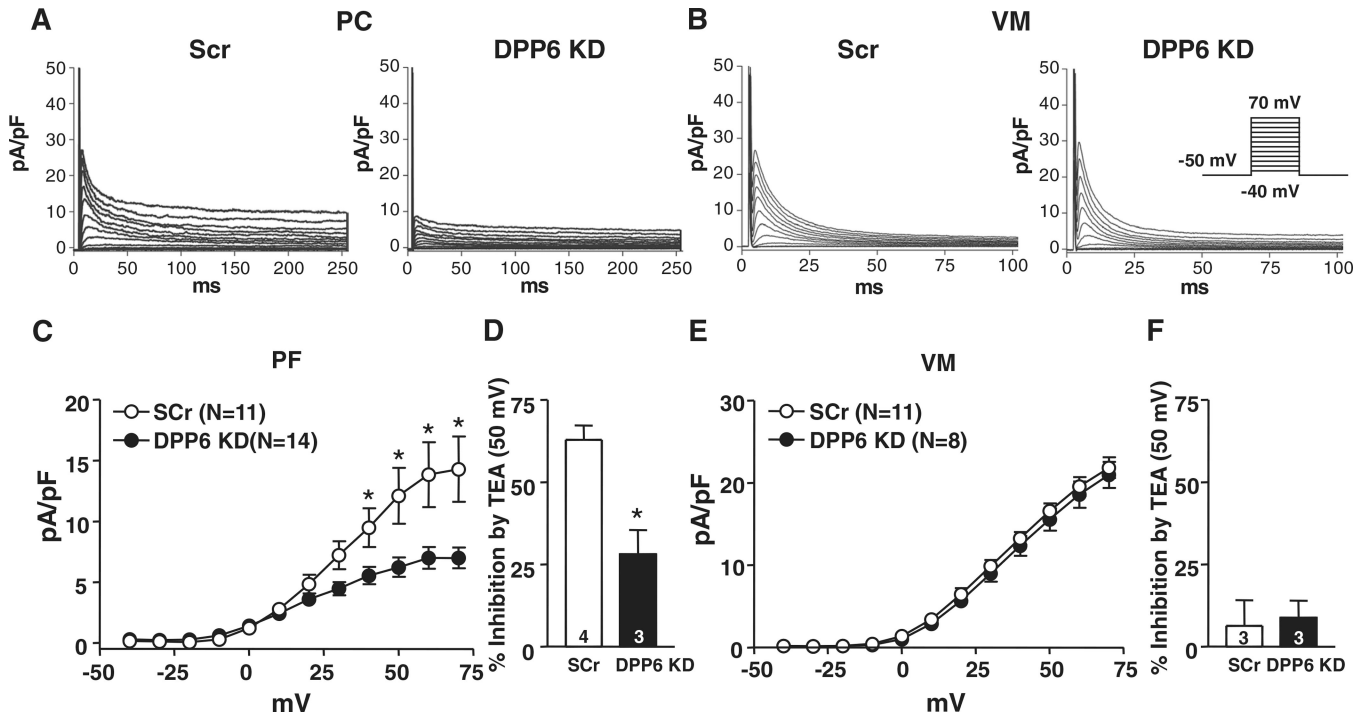
Figure 6. Effects of dipeptidyl peptidase-like protein-6 (DPP6) knockdown (KD) on Purkinje fiber cell (PC) and ventricular myocyte (VM) I_{to}

Examples of Ito recordings from PC **A**, and VM **B**, infected with Adv-GFP-Scr (Scr) or Adv-GFP-DPP6 KD (DPP6 KD). Currents were obtained with 250- (PC) or 100-millisecond (VM) depolarizations at 0.1 Hz. **C** and **E**, Mean±SEM I_{to} density-voltage relations in Scr or DPP6 KD from PCs and VMs. **D** and **F**, Percentage inhibition by 10 mmol/L tetraethylammonium (TEA) of PC (**D**) or VM (**F**) I_{to} at 50 mV. *P<0.05, Scr vs DPP6 KD. GFP indicates green fluorescent protein.
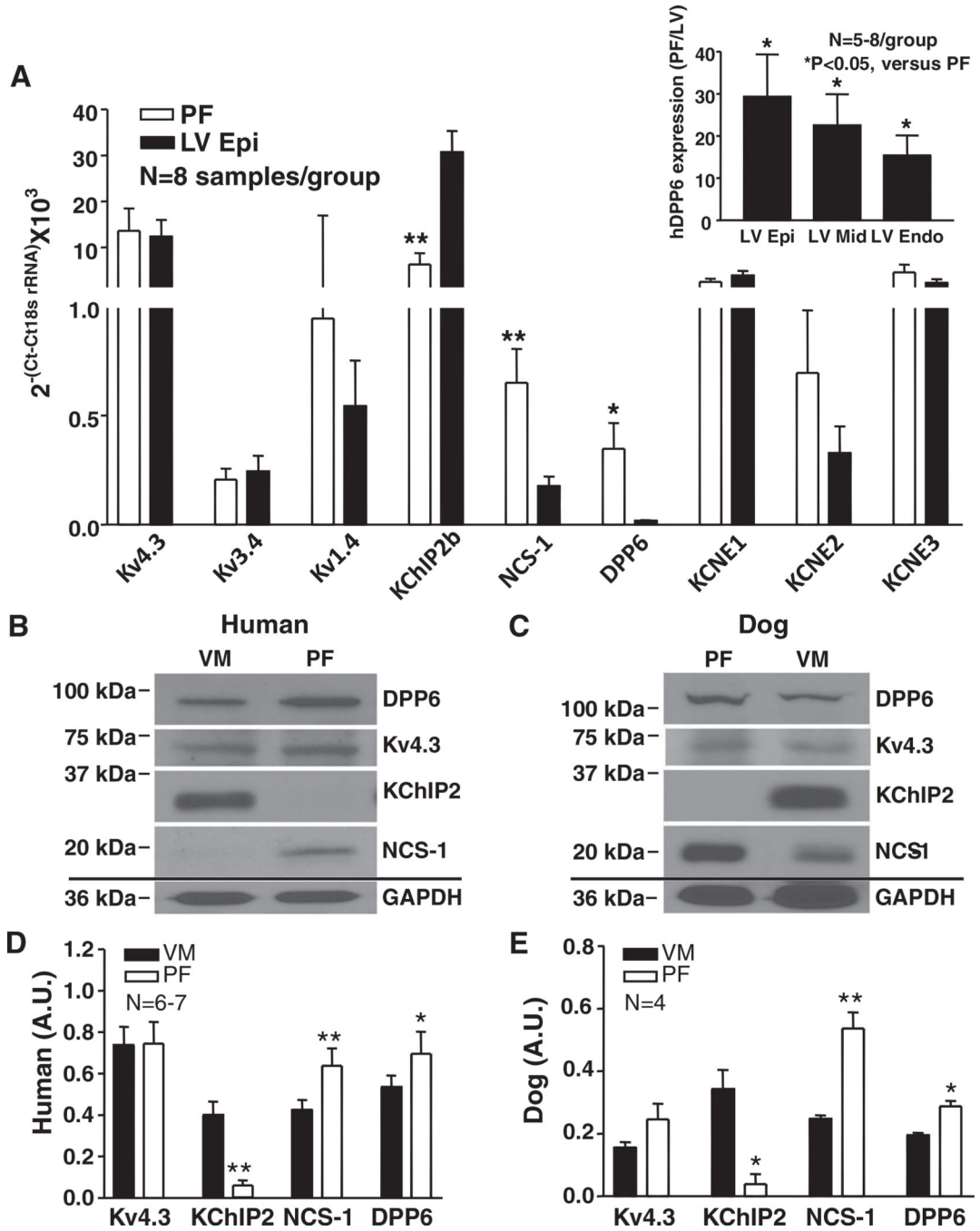
Figure 7. mRNA and protein expression of I_to subunits

A, Ito subunit mRNA expression in human heart. Mean±SEM normalized results for Kv4.3, Kv3.4, Kv1.4, K+-channel interacting protein type-2 (KChIP2)b, neuronal calcium sensor-1 (NCS-1), dipeptidyl peptidaselike protein-6 (DPP6), KCNE1, KCNE2, and KCNE3. *$P<0.05$, **$P<0.01$, Purkinje fibers (PF) vs left ventricle (LV) epicardium (Epi). **Inset**, DPP6 mRNA expression in PF as ratio of LV Epi (n=8), midmyocardium (LV Mid) (n=5), and endocardium (Endo) (n=6). *$P<0.05$, PF vs LV layers. **B** and **C**, Representative Western blot results in ventricular muscle (VM) and PF membrane fractions from human (**B**) and dog

(**C**) hearts. All blots shown were from 1 VM and 1 PF sample on the same membrane for each, which was stripped before each antibody was applied. **D** and **E**, Mean±SEM protein levels normalized to GAPDH. *P<0.05, **P<0.01, PF vs VM.
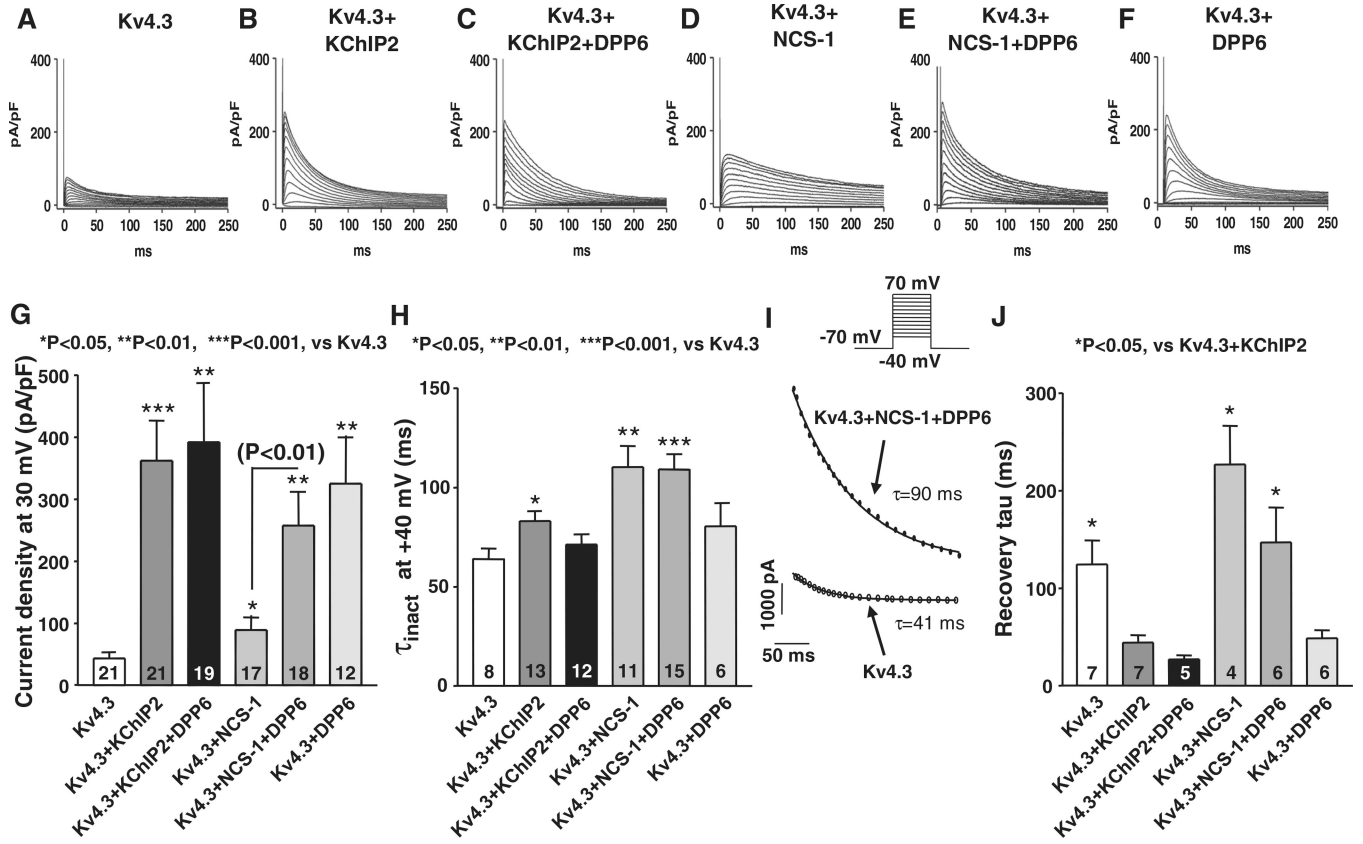
Figure 8. Comparison of I_to properties obtained from different subunit-combinations in heterologous expression system

Examples of currents recorded in Chinese hamster ovary cells transiently transfected with Kv4.3 (**A**), Kv4.3+K+-channel interacting protein type-2 (KChIP2; **B**), Kv4.3+KChIP2+DPP6 (**C**), Kv4.3+neuronal calcium sensor-1 (NCS-1; **D**), Kv4.3+NCS-1+DPP6 (**E**), or Kv4.3+DPP6 (**F**). Currents were recorded during 250-millisecond depolarizations at 0.1 Hz. **G**, Mean±SEM current densities at 30 mV. *$P<0.05$, **$P<0.01$, ***$P<0.001$ vs Kv4.3 only. **H**, Mean±SEM inactivation time constants at 40 mV. *$P<0.05$, **$P<0.01$, ***$P<0.001$ vs Kv4.3 only. **I**, Representative fts from 2 experiments. **J**, Mean±SEM recovery time constants obtained as illustrated in Online Figure VIIIB. *$P<0.05$, vs Kv4.3+KChIP2.